Design, fabrication and characterization of nano-imprinted single mode waveguide structures for intra-chip optical communications

John Justice[a1], Umar Khan[a], Tia Korhonen[b], Arjen Boersma[c], Sjoukje Wiegersma[c], Mikko Karppinen[b], and Brian Corbett[a],

[a]Tyndall National Institute, University College Cork, Lee Maltings, Cork, Ireland[a]
[b]VTT Technical Research Centre of Finland, Oulu, Finland
[c]TNO, De Rondom 1, 5612AP, Eindhoven, The Netherlands

ABSTRACT

In the Information and Communications Technology (ICT) sector, the demands on bandwidth continually grow due to increased microprocessor performance and the need to access ever increasing amounts of stored data. The introduction of optical data transmission (e.g. glass fiber) to replace electronic transmission (e.g. copper wire) has alleviated the bandwidth issue for communications over distances greater than 10 meters, however, the need has arisen for optical data transfer over shorter distances such as those found inside computers. A possible solution for this is the use of low–cost single mode polymer based optical waveguides fabricated by direct patterning Nanoimprint Lithography (NIL). NIL has emerged as a scalable manufacturing technology capable of producing features down to the hundred nanometer scale with the potential for large scale (roll-to-roll) manufacturing.

In this paper, we present results on the modeling, fabrication and characterization of single mode waveguides and optical components in low-loss ORMOCER™ materials. Single mode waveguides with a mode field diameter of 7 μm and passive structures such as bends, directional couplers and multi-mode interferometers (MMIs) suitable for use in 1550 nm optical interconnects were fabricated using wafer scale NIL processes. Process issues arising from the nano-imprint technique such as residual layers and angled sidewalls are modeled and investigated for excess loss and higher order mode excitation. Conclusions are drawn on the applicability of nano-imprinting to the fabrication of circuits for intra-chip/board-level optical interconnect.

Keywords: Optical interconnect, On-board, intra-chip, nanoimprint lithography, single mode waveguide

1. INTRODUCTION

Moore's law, which suggests that the number of transistors in integrated circuits will double every two years, is well known in the information and communication technology sector and its repercussions are well documented. Other factors are now placing limits on processor performance. One example of this is the increasing power of supercomputers which is growing by a factor of 10 every 4 years.[1] The additional computation associated with this is placing an increased demand in the transfer of data from the processor to the memory chips and to the edge of the board/rack in data centers. On-board and intra chip communications inside computers is currently implemented using metal interconnects which have inherent limitations in power, signal distortion, crosstalk and limited pin-out density as higher frequencies are used.[2] Optical signaling is less affected by these issues, which has resulted in it being the preferred approach to high bandwidth transfer at distances greater than 10 meters. The demand now is for optical communications to move into the computer and onto the board enabling high bandwidth connections between processor, memory and externally to long haul fiber, Figure 1(a). A suitable technology must be capable of high volume production and of low cost. Nano-imprint lithography of polymer optical waveguide provides a possible solution[3], [4] .

The FIREFLY project aims to address this through the development of a single mode waveguide platform at 1300 and 1550 nm using Ultra Violet (UV) Nano-Imprint lithography (Figure 1(b)). Embedded Vertical Cavity Surface Emitting

[1] John.justice@tyndall.ie www.tyndall.ie , www.fp7-firefly.eu

Optical Interconnects XV, edited by Henning Schröder, Ray T. Chen, Proc. of SPIE Vol. 9368, 93680Y · © 2015 SPIE · CCC code: 0277-786X/15/$18 · doi: 10.1117/12.2078974

Lasers (VCSELs) are driven by on-board electronic circuitry with the optical signal coupled into the waveguides using integrated turning mirrors. The signal is then routed and manipulated as required on-board and then coupled to either single mode fibers for long haul communication or on-board photoreceivers. The use of single mode waveguides permits the integration with single mode fibers and silicon photonics enabling dense wavelength division multiplexing (DWDM).

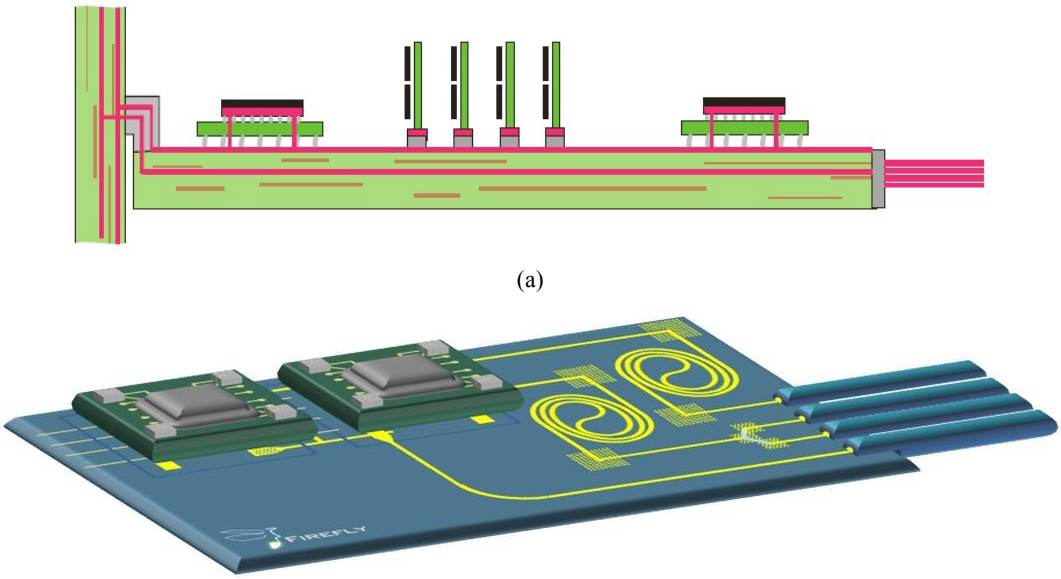

(a)

(b)

Figure 1. (a) Concept of intra-chip interconnect for use in data-centers and intra-chip communications. Single mode fibers are connected to the board and signals routed to processors/memory chips.[5] Optical pathways are shown in pink. (b) Firefly concept for the implementation of an on-board nano-imprinted single mode optical interconnect which facilitates direct communication between Vertical Cavity Surface Emitting Lasers and external single mode fibers. Optical waveguides are shown in yellow.

2. FABRICATION OF NANOIMPRINTED WAVEGUIDES

Single mode waveguide stacks have been fabricated by UV Nano-imprint lithography of polymer materials on 4" diameter silicon wafers. The polymers used were commercially available Ormocer materials[6]; Ormocore with a refractive index of n=1.535 at 1550 nm and Ormoclad with a refractive index of n = 1.521 at 1550 nm. The refractive index of the core and cladding materials can be tuned by appropriate mixing of these two materials prior to fabrication in order to give the required core refractive indices. The nano-imprint process broadly consists of two steps; the formation of the stamp and the nano-imprint lithography. The stamp is formed by lithographic patterning of positive photoresist. A photoresist pattern is transferred to an Ormocer-coated glass wafer by an initial UV nanoimprint step. This glass wafer, which is a negative image of the original pattern, is coated with anti-adhesion coating and is then used to form the waveguides. The use of photoresist in the mastering results in smooth sidewalls for the waveguide with minimal scattering and with optical loss dominated by material attenuation.[7] Both inverted rib and ridge type waveguide processes have been used. The inverted rib waveguide process is outlined in Figure 2. The lower cladding material is applied by spin-coating of Ormoclad to a thickness of 30 µm. The 30 µm thickness in the cladding is to ensure optical isolation between the waveguide mode and the underlying substrate Figure 2(1). The nanoimprint stamp is brought into contact with the polymer which is conformally distorted to match its shape. Broadband Ultra Violet (UV) illumination cures this cladding material resulting in trenches which mirror the stamp upon its release, Figure 2(3). These trenches are filled by material of a higher refractive index, Ormocore, which is applied via spin-coating, resulting results in the formation of a slab layer of higher index material above the trench. This thickness of this slab can be well controlled by tuning the material viscosity and the spin-coating parameters. This slab or "residual layer" has a thickness which is typically less than 0.5 µm, shown in in Figure 2(5). The core material is hardened under UV illumination. The final step

is the application of an over-layer of lower index material to form the top cladding of the waveguide. Ormoclad is applied by spin coating a layer of 30 µm thickness. The waveguide is therefore composed of 5 µm square trench of higher index material clad by two 30 µm thick layers of lower index material. The index contrast between the core and cladding has been designed to be 0.6%.

A ridge process begins with application of the underlying lower index Ormoclad cladding material by spin-coating and curing. The higher index Ormocore core material is applied and an imprint stamp forms a ridge waveguide which is cured. The upper cladding is then spin-coated and cured. The features in the imprint stamp for the ridge process must obviously be inverted compared to the trench process detailed above.

In subsequent sections, bend samples were made using the inverted method, but the same results were confirmed with ridge process. Directional couplers were made using both methods with similar results. For MMI, the ridge process gave better result in the first trials.

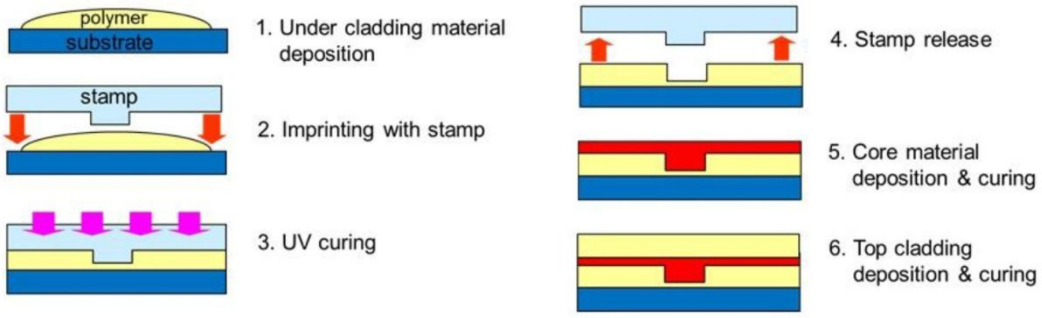

Figure 2. Fabrication process for inverted rib waveguides using UV nanoimprinting.

3. DESIGN OF POLYMER WAVEGUIDES

The polymer waveguides were designed with 5 x 5 µm square waveguides using an index contrast of 0.6% between the core and cladding polymers with n=1.528 and n=1.519 respectively. The choice of this low index contrast means that waveguide supports only the fundamental waveguide mode at 1550 nm with a Mode Field Diameter (MFD) of approximately 7 µm where the MFD is defined at $1/e^2$ of the electric field. This MFD is chosen to be intermediate between the 4-5 µm MFD of the VCSEL sources used and standard single mode fibers which have MFD of approximately 10 µm and thus maximizes their coupling. The VCSELS are similar to those described by Ortsiefer et al.[8]

The routing of signals requires in-plane bending of the waveguides. The low contrast in refractive indices between the core and cladding of 0.6% and the resultant low optical confinement places a lower limit on the bend radius. If the bend radius is too small the light escapes the waveguide core and radiates out into the cladding causing high optical losses. Bends of large radii have two disadvantages; firstly the loss due to the length of the waveguide will be higher, and secondly, will require a large footprint on the substrate. The loss of the waveguides has previously been measured from the attenuation of the optical signal in a long spiral of length 27 cm. The overall loss was measured as 0.84-0.89 dB/cm at 1530 nm and 0.75-0.8 dB/cm at 1550 nm , composed of material loss as circa 0.7 dB/cm at 1530 nm and 0.6 dB/cm at 1550 nm (from material datasheet) and therefore an excess waveguide loss of <0.2 dB/cm in a straight waveguide. The loss measurements and part of the results were described earlier by Korhonen et al [9].

The simulations of modal structure of the waveguides used a commercially available 3D mode solver, FIMMWAVE from Photon design.[10] The excess loss of the waveguides at various bend radii was simulated. The effect of residual layer was included in the simulation by the introduction of a slab of core material of thickness varying from 0 to 1.0 µm in 0.5 µm steps. The bend losses at radii less than 10 mm are predicted to increase significantly for residual layer thicknesses >1 µm in a 5 micron core. Simulations in Figure 3(a) shows that in order to keep bend losses <3 dB for 120° S-bends composed of two 60° arc segments, it is required to keep the bend radius greater than 8 mm and residual layer thickness to less than <0.5 µm.

Waveguide bends of radii from 2 to 10 mm were fabricated on 4" silicon wafers employing these S-bends. The excess loss in the bend structures was measured in comparison to straight control waveguides fabricated on the same chip. The measurements were repeated from three sample chips, each having the same layout. A good match between simulated and measured excess loss was observed, Figure 3 (b). The measured loss increases rapidly for bend radii <7 mm with minimal increases for bend radii greater than 8 mm. The residual layer thickness was measured via microscope imaging to be approximately 0.5 µm.

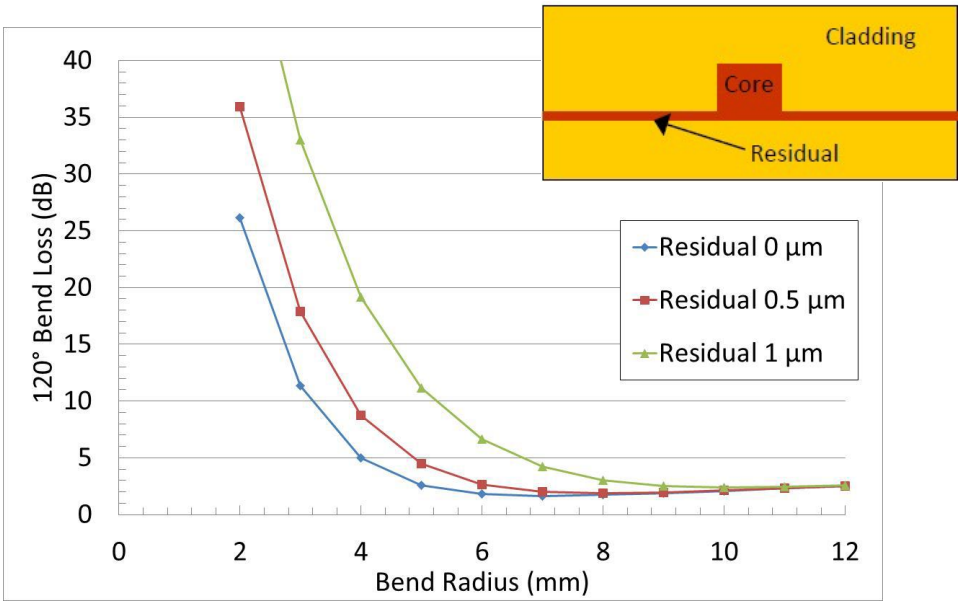

(a)

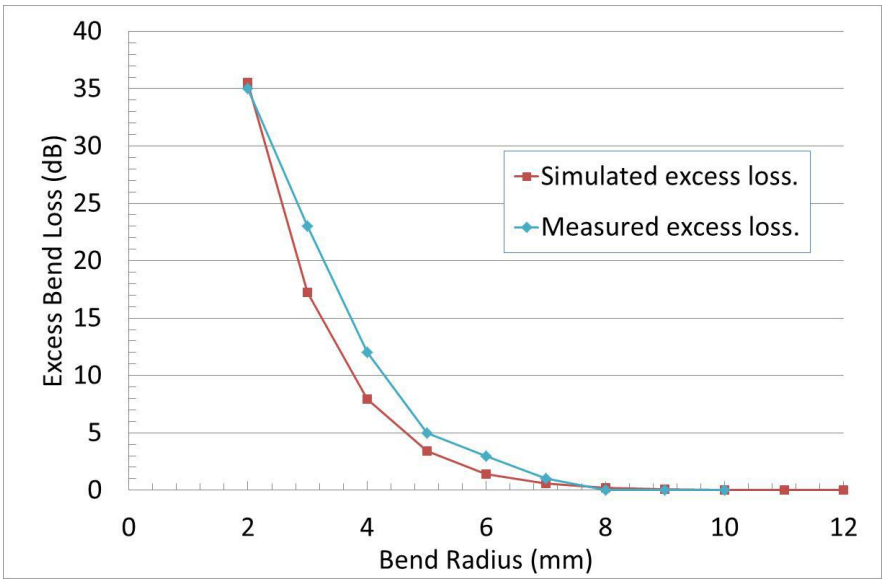

(b)

Figure 3. (a) Simulation of bend loss with increasing residual layer thickness (schematic of waveguide with residual layer shown inset). (b) Comparison of simulation and measurement for excess bend loss in an S-bend (2x 60° arcs) when compared to straight control waveguide. Lines are shown as guide to eye.

4. PASSIVE OPTICAL COMPONENTS

On-board optical interconnect should include optical components capable of functions beyond the simple routing of signals. Manipulation of optical signals, such as splitting of light, wavelength multiplexing, polarisation selection and other functions may be implemented by the inclusion of passive optical components such as multi-mode interference (MMI) devices and directional couplers. Both of these devices have been fabricated on 4" Silicon wafers. Device characteristics have been measured and compared with simulations.

4.1 Multimode Interference Devices

Multi-mode interference devices are passive components which employ self-imaging in a multi-mode section of waveguide[11]. In section of the waveguide capable of supporting higher order modes, the input field is reproduced in single or multiple images at intervals along the direction of propagation of the waveguide. This self-imaging occurs at lengths given from

$$L_N = \left(\frac{p}{N}\right) \times \frac{3}{4} L_\pi \tag{1}$$

where p=0, 1, 2, 3.. is an integer, N is the number of images and L_π is the beat length of the two lowest order modes,

$$L_\pi = 4 \times N_{Eff} \times W_{Eff}{}^2 \big/ 3\lambda \tag{2}$$

where N_{Eff} is the effective refractive index of the waveguide, W_{Eff} is the effective width of the multi-mode region and λ is the wavelength (1.55 μm). We have chosen an MMI design employing the single mode input and output waveguide as described, and a multi-mode region of 40 μm width. This width keeps the coupling length to less than 1 mm with simulations of a 1 x 2 splitter predicting a peak efficiency of approximately 90% at a length of 970 μm. The gap between the output waveguides is 16.5 μm. The inclusion of tapers at the start of the output waveguides was considered, however simulation showed no significant increase in coupling associated with their inclusion. This is attributable to the relative large MFD of 7 micron and low index contrast. The situation is different in material systems with high index contrasts between core and cladding such as Silicon and III-V MMI devices where modes and more tightly confined and tapering improves the efficiency. The excitation of higher order modes and reconstitution of N-fold beats are shown in Figure 4 which is a plan view of the simulated electric field intensity. MMIs were fabricated by NIL with lengths varied from 880 μm to 980 μm in 20 μm steps in order to measure the variation in coupling efficiency.

The devices were measured on a waveguide measurement system using a fiber-coupled tunable laser source. Single mode lensed fibers are coupled to the input and output waveguides of the MMI and the power maximized. The efficiency is calculated as the sum of both outputs divided by the total output power through an adjacent straight waveguide which is used as a control. The measured efficiencies for MMIs of different lengths are shown in Figure 5 and demonstrate a good match with the simulation with the efficiency increasing with the length of the multimode region to a maximum of approximately 970 μm.

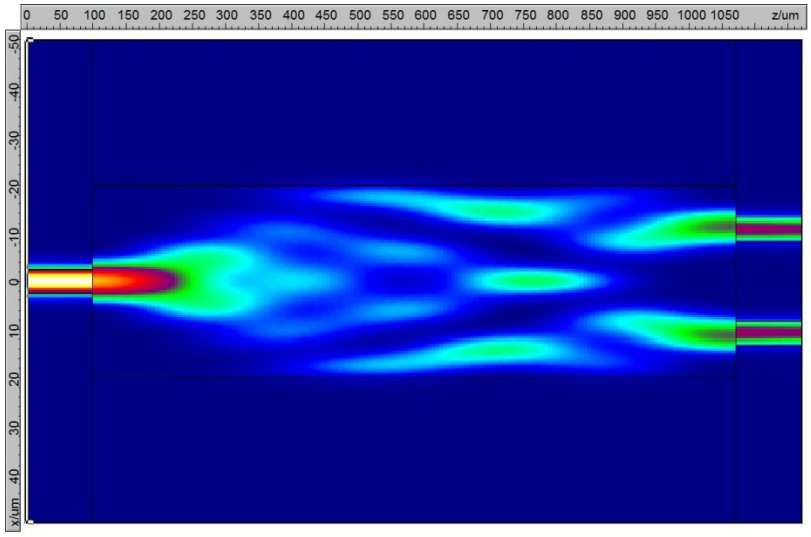

Figure 4. Simulation showing the field intensity in a 1x2 MMI splitter using 5 µm square single mode waveguides for input and outputs and a 40 µm multi-mode region.

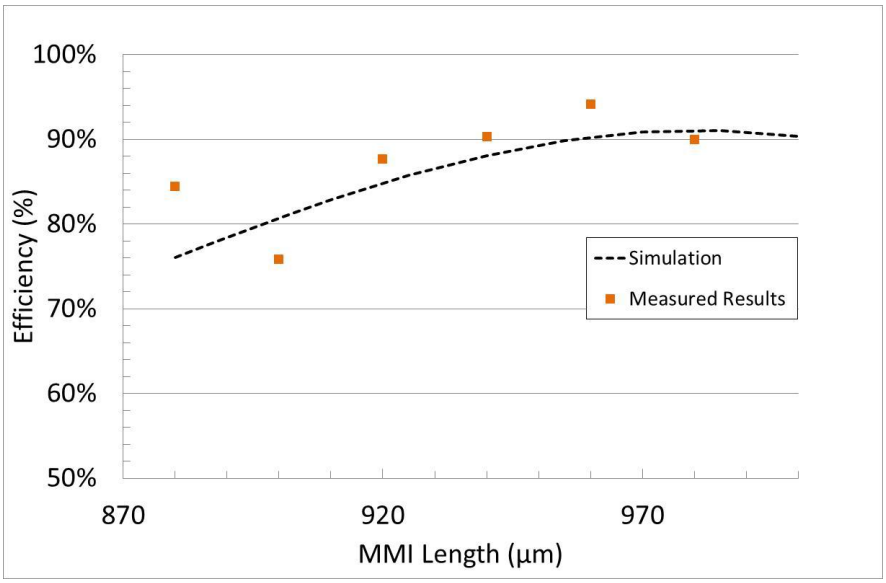

Figure 5. Measured efficiency of polymer MMIs versus length of multi-mode region as compared to simulations.

4.2 Directional Couplers

Directional couplers were also investigated. Directional couplers operate on the principle of resonant power transfer between two adjacent waveguides whose modes overlap. Maximum power is transferred under the following conditions; the two waveguides are in close proximity separated by a gap, d, which is comparable to the wavelength of operation, the waveguides have the same propagation constant and the waveguides have an interaction length, L, equal to the coupling length.

The amount of light split between waveguides can be chosen by varying the length of the interaction region. The gap between waveguides has been chosen as d=5 µm for two reasons. Firstly, gaps less than 2 µm are difficult to fabricate given the waveguide feature size of 5 µm and, secondly, coupling lengths for widths greater than 8 µm are large and greater than the planned demonstrator chip size of 2 cm x 2 cm. Demonstrators have been fabricated by NIL on 4" Silicon wafers with interaction lengths varying from 500 µm to 5000 µm in 500 µm steps to allow measurement of the

power exchange between coupled waveguides. The input waveguide spacing is 40 µm centre-to-centre to eliminate crosstalk between the two input / output waveguides. The two input and output waveguides are brought into proximity using S-bend sections of 1000 µm in length with bend radii equal to 10 mm with minimal bend loss. Some coupling does occur between waveguides before the 5 µm spaced interaction region due to the closeness of the waveguides at the end of the S-bends. This can be seen in simulations in Figure 6 (a) where the light in the input waveguide ("through") is less than 100% at a length of 0 µm due to some of it having being already coupled into the coupled waveguide ("coupled"). Simulations predict a coupling length, where all the light input from one waveguide is coupled to the adjacent waveguide, of 2000 µm when the previously described waveguides at separated by 5 µm spacing.

Measurements were carried as per the MMIs. Laser output is coupled to the input of the directional couplers using lensed fibers. The output power from the through and coupled waveguides was then measured. The total output was normalized to the input for directional couplers of different lengths. The fabricated directional couplers display a coupling length of slightly less than 2000 µm as shown in Figure 6 (b).

4.3 Tolerance to processing issues

The use of polymers in nano-imprint lithography results two parasitic effects; the presence of a residual layer of core material as described previously, and sloped side walls on the waveguides. These are shown schematically in Figure 7(a) with a microscope image of actual imprinted waveguide shown in Figure 7(b). Processing of polymers may also result in a variation in the actual refractive index contrast between the core and cladding materials. Simulations have been used to investigate the effect of these variations and shown that directional couplers are much more sensitive as compared to MMI devices. Sloped sidewalls reduce the effective gap between waveguides and thus reducing the coupling length in directional couplers. Thinner residual layer increases the coupling length by increasing the effect index contrast between adjacent waveguides and thereby increasing the modal confinement and reducing the overlap. Errors in mixing ratios of the polymers can also affect index contrast between core and cladding. MMI devices, whose modal expansion occurs in the core material, do not depend on the overlap of the evanescent tail of mode into an adjacent waveguide and therefore are less affected by the changes in refractive index contrast than directional couplers. The increase in effective width due to sloped sidewalls is negligible if the MMI width is sufficiently large. The MMIs are therefore more tolerant to all these process related effects.

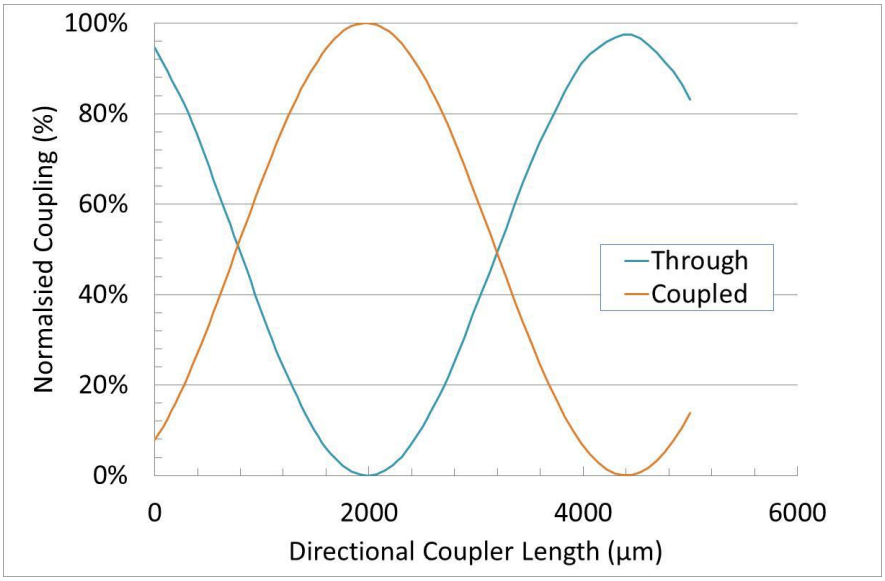

(a)

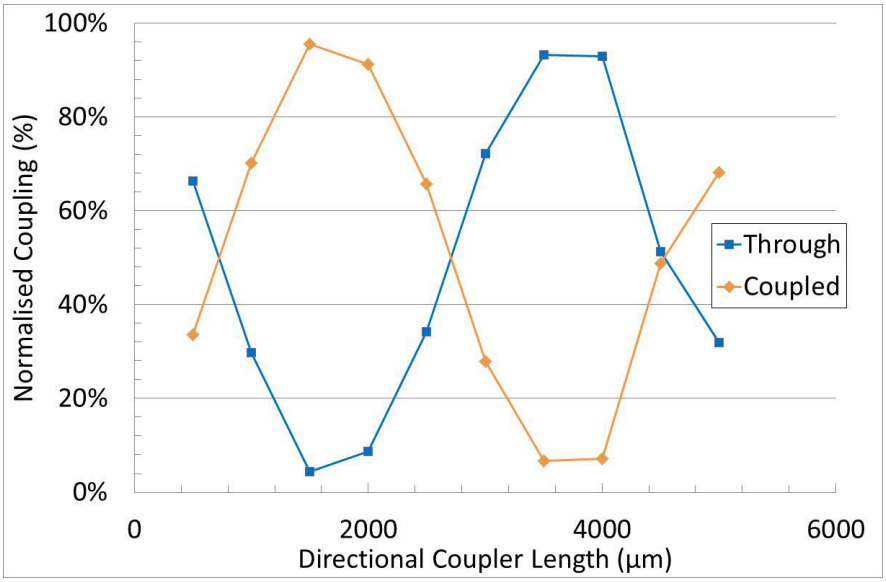

(b)

Figure 6. (a) Simulation of normalized power in waveguides of directional coupler versus propagation length for input "through" branch (blue) and "coupled" branch (orange) and (b) measured results (lines are shown as guide to eye).

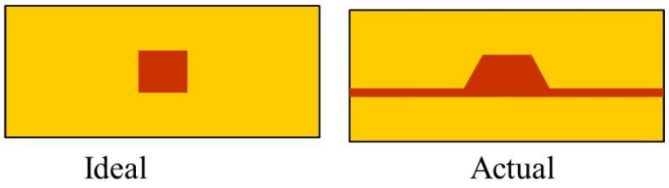

(a)

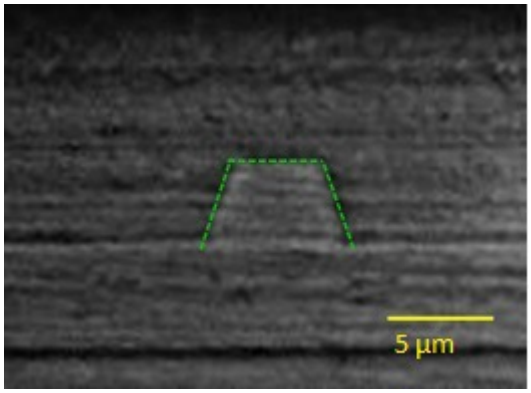

(b)

Figure 7. (a) Process related difference between ideal and actually imprinted waveguide. (b) Microscope image of actual waveguide.

5. CONCLUSIONS

The FIREFLY project is addressing the growing need for low cost, manufacturable on-board optical interconnect using polymeric waveguides fabricated by UV nano-imprint lithography. Single mode waveguides with a refractive index contrast of 0.6% between the core and cladding have been fabricated using commercially available Ormocer materials. These waveguides support single mode operation at 1550 nm with a MFD of approximately 7 µm in a 5 µm square core. Waveguide bends and passive optical devices such as MMIs and directional couplers have been simulated, fabricated on 4" Silicon wafers and characterized with resulting good agreement between simulation and measurement. The nano-imprint lithography process can result in variations in the residual layer thickness, sloped sidewalls and different contrast in the refractive indices. Simulations have shown than MMIs are less susceptible to these variations than directional couplers. Design of future on-board interconnect using imprinted polymeric waveguide should take account of the tolerance of different passive optical components to these variations to maximize reproducibility of performance.

We would like to acknowledge Noora Salminen[b] and Annukka Kokkonen[b] for their work on the optical characterisation of the bend and spiral samples.

REFERENCES

[1] Pepeljugoski, P., Kash, J., Doany, F., Kuchta, D., Schares, L., Schow, C., Taubenblatt, M., Jan Offrein, B., Benner, A., "Low Power and High Density Optical Interconnects for Future Supercomputers," OSA Optical Fiber Communication Conference (OFC2010), paper OThX2, (2010).

[2] Miller, D.A.B. ,Ozaktas, H.M., "Limit to the Bit-Rate Capacity of Electrical Interconnects from the Aspect Ratio of the System Architecture," Journal of Parallel and Distributed Computing, 41(1), 42–52 (1997).

[3] Chou,S.Y., Krauss, P.R. and Renstrom, P.J., "Imprint of sub-25 nm vias and trenches in polymers," Applied Physics Letters 67(21), 3114-3116 (1995).

[4] Guo, L.J., "Recent progress in nanoimprint technology and its applications," J. Phys. D Appl. Phys., 37(11), R123-R141 (2004).

[5] Offrein, B. "Silicon Photonics for optical interconnects in computing applications," 2012 Photonics Europe, Session 8, Industry and Silicon Photonics, 8431-32(2012).

[6] Information on Ormocer™ Materials, Ormocore™ and Ormoclad™ available at http://www.microresist.de/products/ormocers/pdf/pi_ormocore_clad_en_07062201_ls_neu.pdf

[7] Hiltunen, J., Hiltunen, M., Puustinen, J, Lappalainen, J, Karioja, P., "Fabrication of optical waveguides by imprinting: usage of positive tone resist as a mould for UV-curable polymer," Optics Express, 7 (25), 22813-22822 (2009).

[8] Ortsiefer, M., Rosskopf, J., Kogel, B., Daly, A., Gorblich, M., Xu, Y., Greus, C., Neumeyr, C., "Long Wavelength VCSELs with Enhanced Temperature and Modulation Characteristics," Semiconductor Laser Conference (ISLC) 2014 International, 74-75, 7-10 Sept. 2014.

[9] Korhonen, T., Salminen, N., Kokkonen, A., Masuda, N., and Karppinen M., "Multilayer single-mode polymeric waveguides by imprint patterning for optical interconnects," Proc. SPIE 8991, Optical Interconnects XIV, 899103 (2014).

[10] Fimmwavee™ by Photon design. Available: http://www.photond.com/products/fimmwave.htm

[11] Soldano, L.B., Pennings, E.C.M., "Optical multi-mode interference devices based on self-imaging: principles and applications," Journal of Lightwave Technology, 13(4), (1995).